Macrophages retain hematopoietic stem cells in the spleen via VCAM-1

Partha Dutta,[1] Friedrich Felix Hoyer,[1] Lubov S. Grigoryeva,[1] Hendrik B. Sager,[1] Florian Leuschner,[2,3] Gabriel Courties,[1] Anna Borodovsky,[4] Tatiana Novobrantseva,[4] Vera M. Ruda,[4] Kevin Fitzgerald,[4] Yoshiko Iwamoto,[1] Gregory Wojtkiewicz,[1] Yuan Sun,[1] Nicolas Da Silva,[1] Peter Libby,[5] Daniel G. Anderson,[6,7,8,9] Filip K. Swirski,[1] Ralph Weissleder,[1,10] and Matthias Nahrendorf[1]

[1]Center for Systems Biology, Massachusetts General Hospital and Harvard Medical School, Boston, MA 02114
[2]Department of Cardiology, Medical University Hospital Heidelberg, D-69120 Heidelberg, Germany
[3]DZHK (German Centre for Cardiovascular Research), partner site Heidelberg/Mannheim, D-69120 Heidelberg, Germany
[4]Alnylam Pharmaceuticals, Cambridge, MA 02142
[5]Cardiovascular Division, Department of Medicine, Brigham and Women's Hospital, Boston, MA 02115
[6]David H. Koch Institute for Integrative Cancer Research, [7]Department of Chemical Engineering, and [8]Institute for Medical Engineering and Science, Massachusetts Institute of Technology, Cambridge, MA 02142
[9]Division of Health Science Technology, Harvard University and Massachusetts Institute of Technology, Cambridge, MA 02139
[10]Department of Systems Biology, Harvard Medical School, Boston, MA 02115

Splenic myelopoiesis provides a steady flow of leukocytes to inflamed tissues, and leukocytosis correlates with cardiovascular mortality. Yet regulation of hematopoietic stem cell (HSC) activity in the spleen is incompletely understood. Here, we show that red pulp vascular cell adhesion molecule 1 (VCAM-1)$^+$ macrophages are essential to extramedullary myelopoiesis because these macrophages use the adhesion molecule VCAM-1 to retain HSCs in the spleen. Nanoparticle-enabled in vivo RNAi silencing of the receptor for macrophage colony stimulation factor (M-CSFR) blocked splenic macrophage maturation, reduced splenic VCAM-1 expression and compromised splenic HSC retention. Both, depleting macrophages in CD169 iDTR mice or silencing VCAM-1 in macrophages released HSCs from the spleen. When we silenced either VCAM-1 or M-CSFR in mice with myocardial infarction or in ApoE$^{-/-}$ mice with atherosclerosis, nanoparticle-enabled in vivo RNAi mitigated blood leukocytosis, limited inflammation in the ischemic heart, and reduced myeloid cell numbers in atherosclerotic plaques.

CORRESPONDENCE
Matthias Nahrendorf:
mnahrendorf@mgh.harvard.edu
OR
Partha Dutta:
dutta.partha@mgh.harvard.edu

Abbreviations used: DT, diphtheria toxin; GMP, granulocyte-macrophage progenitor; HSC, hematopoietic stem cell; HSPC, hematopoietic stem and progenitor cell; LSK, lineage$^-$ Sca-1$^+$ c-Kit$^+$ cell; M-CSFR, receptor for macrophage colony stimulating factor; MI, myocardial infarction; VCAM-1, vascular cell adhesion molecule 1; VLA-4, very late antigen-4.

Leukocytosis correlates closely with cardiovascular mortality. In the steady state, blood leukocytes derive exclusively from bone marrow hematopoietic stem cells (HSCs). Supporting cells (Sugiyama et al., 2006; Ding et al., 2012; Ding and Morrison, 2013), including macrophages (Winkler et al., 2010; Chow et al., 2011), maintain the bone marrow HSC niche and regulate hematopoietic stem and progenitor cell (HSPC) activity by supplying various cytokines and retention factors. Systemic inflammation can stimulate extramedullary hematopoiesis in adult mice and humans. Splenic myelopoiesis supplies inflammatory monocytes to atherosclerotic plaques (Robbins et al., 2012) and the ischemic myocardium (Leuschner et al., 2012). In ischemic heart disease, HSPCs emigrate from the bone marrow, seed the spleen, and amplify leukocyte production (Dutta et al., 2012). Splenic HSPCs localize in the red pulp near the sinusoids in parafollicular areas (Kiel et al., 2005). Likewise, after adoptive transfer of GFP$^+$ HSPCs, GFP$^+$ colonies populate the splenic red pulp of atherosclerotic ApoE$^{-/-}$ mice (Robbins et al., 2012). During myocardial infarction (MI), proinflammatory monocytes derived from the spleen accelerate atherosclerotic progression (Dutta et al., 2012). Collectively, these data suggest that splenic myelopoiesis has promise as a therapeutic target; however, the components of the splenic hematopoietic niche are incompletely

The Rockefeller University Press $30.00
J. Exp. Med. 2015 Vol. 212 No. 4 497–512
www.jem.org/cgi/doi/10.1084/jem.20141642

understood, especially compared with the well-studied bone marrow niche. Understanding HSC retention factors and their regulation in the spleen was the purpose of this study.

Because the spleen harbors very few HSCs in the steady state, we investigated the splenic hematopoietic niche after injecting the Toll-like receptor ligand LPS to activate extramedullary hematopoiesis. In the bone marrow, macrophages are an integral part of the HSC niche (Winkler et al., 2010; Chow et al., 2011) and differentiation depends on the receptor for macrophage colony-stimulating factor (M-CSFR, CD115; Auffray et al., 2009). We thus hypothesized that splenic hematopoietic niche assembly also requires M-CSFR signaling. In line with knockout studies (Takahashi et al., 1994; Dai et al., 2002), in vivo knockdown of M-CSFR with nanoparticle-encapsulated siRNA reduced splenic macrophage numbers substantially. Interestingly, decreased macrophage numbers were associated with a reduction of splenic HSCs. Depleting macrophages with diphtheria toxin (DT) in CD169 iDTR mice reproduced the findings obtained with M-CSF–directed siRNA treatment, thereby indicating that macrophages have a key role in splenic HSC maintenance. To investigate how splenic macrophages retain HSCs, we measured changes in splenic expression of major bone marrow retention factors after M-CSFR silencing. Silencing M-CSFR selectively reduced splenic VCAM-1, and the adhesion molecule was primarily expressed by macrophages. Inhibiting macrophage expression of VCAM-1 with siRNA targeting this adhesion molecule reduced splenic HSPC numbers. Finally, we found that M-CSFR and macrophage-directed VCAM-1 silencing in mice with atherosclerosis mitigated blood leukocytosis and dampened inflammation in atherosclerotic plaques and the infarcted myocardium. These data reveal the importance of VCAM-1 expression by splenic macrophages for extramedullary hematopoiesis and illustrate the therapeutic potential of RNAi as an antiinflammatory that mutes emergency overproduction and provision of myeloid cells.

RESULTS

M-CSFR (CD115) knockdown attenuates LPS-induced splenomegaly

Several siRNA sequences targeting the M-CSF receptor were selected using in silico prediction methods (Dahlman et al., 2014) and tested in vitro at two concentrations in M-CSFR–expressing cells. The six best duplexes (Fig. 1 A) underwent further testing at seven dilutions (Fig. 1 B). The siRNA with the best in vitro silencing at low concentrations (siCD115; sense, cuAcucAAcuuucuccGAAdTsdT; anti-sense, UUCGGAGAAAGUUGAGuAGdTsdT) was incorporated into lipidoid nanoparticles (Love et al., 2010) for in vivo studies. These nanoparticles exhibit particular efficiency for in vivo silencing in monocytes and macrophages after systemic delivery (Leuschner et al., 2011; Novobrantseva et al., 2012; Majmudar et al., 2013; Courties et al., 2014) and resemble siRNA delivery vehicles currently used in clinical studies (Coelho et al., 2013). siCD115 was tested for in vivo silencing in the spleen, which has the highest siRNA concentration after systemic injection of nanoparticle carriers (Leuschner et al., 2011). Because the adult steady-state spleen harbors only a few HSPCs, we induced extramedullary hematopoiesis by treating mice with LPS. Mice then received injections of either siCD115 or control siRNA with an irrelevant sequence (siCON), both encapsulated in similar lipidoid delivery nanoparticles (Fig. 1 C). We found that two intravenous siCD115 injections reduced CD115 mRNA levels in splenic monocytes and macrophages by eightfold (Fig. 1 D) and led to a substantial (>75%) in vivo protein knockdown in leukocytes (Fig. 1 E). Although the treatment did not significantly change body weight (Fig. 1 F), LPS-induced splenomegaly (Fig. 1 G) and splenic cell content (Fig. 1 H) fell significantly after siCD115 treatment. Moreover, siCD115 treatment significantly reduced serum IFN-γ levels (Fig. 1 I). Consistently, CD115 knockdown reduced numbers of total blood monocytes and Ly-6c^{high} monocytes in LPS-challenged mice (Fig. 1, J and K).

M-CSFR knockdown decreases splenic HSPC numbers

Next, we enumerated splenic Lin$^-$ Sca-1$^+$ ckit$^+$ CD48$^-$ CD150$^+$ HSCs, LSKs (Lin$^-$ Sca-1$^+$ ckit$^+$ cells), and granulocyte-macrophage progenitors (GMPs) (Lin$^-$ Sca-1$^+$ ckit$^+$ CD16/32^{high} CD34^{high}). The naive mouse spleen contained few hematopoietic stem and progenitor cells (HSCs, 666 ± 166; LSKs, 3,400 ± 1,030; GMPs, 1,300 ± 337 per spleen; Fig. 2, A and B). LPS treatment increased these numbers 30-, 39- and 33-fold, respectively. In parallel to the observation that RNAi curbed LPS-induced splenomegaly, we found that siCD115 treatment decreased splenic HSC, LSK, and GMP numbers significantly (Fig. 2, A and B). Similarly, M-CSFR knockdown reduced bone marrow HSPC numbers (Fig. 2 C). Because CD115 signaling contributes to macrophage survival (Shaposhnik et al., 2010), we investigated whether the receptor has a similar effect on HSCs. CD115 knockdown did not affect HSC and LSK apoptosis in the bone marrow (Fig. 2 D) and spleen (Fig. 2 E).

Splenic niche maintenance requires M-CSFR signaling

To explore how M-CSFR knockdown reduced splenic HSPC numbers, we assessed HSPC proliferation using an in vivo BrdU incorporation assay, as M-CSF may facilitate cell proliferation. However, BrdU incorporation by HSPCs did not differ among the treatment groups, indicating that siCD115 does not change HSPC proliferation rates (Fig. 3 A). Because BrdU may act as a mitogen (Takizawa et al., 2011), we also used a CFSE dilution assay to measure LSK proliferation (Fig. 3 B). For this assay, we sorted LSKs from CD45.1$^+$ mice, labeled them with CFSE, and transferred them into LPS-primed CD45.2$^+$ mice treated with either siCD115 or siCON. Transferred CFSE-labeled LSKs diluted the dye at similar rates in both treatment cohorts, indicating similar rates of LSK proliferation, but the total number of splenic BrdU$^+$ HSPCs declined after siCD115 treatment, reflecting reduced HSPC retention in the splenic niche (Fig. 3 A).

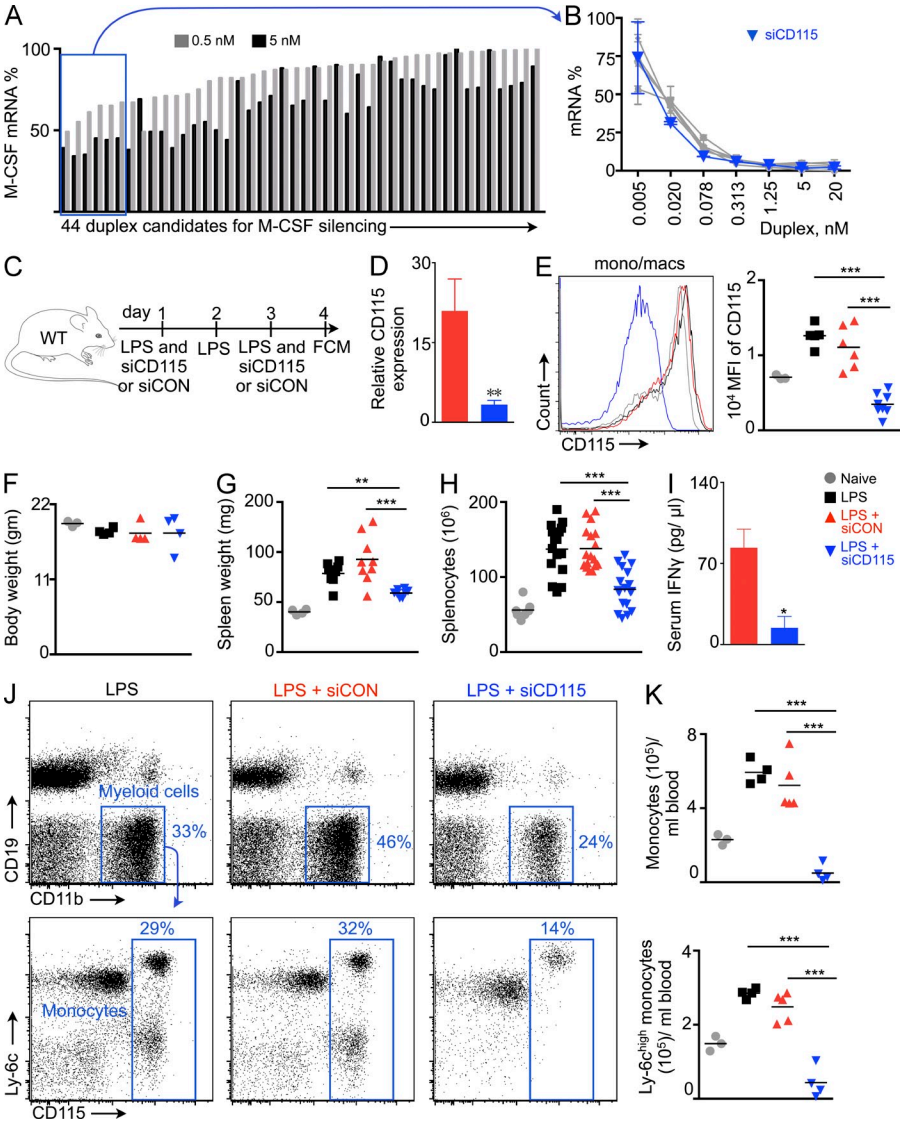

Figure 1. M-CSFR (CD115) knockdown reduces LPS-induced splenomegaly. (A) In vitro screening for siRNA inhibitors of CD115 mRNA (n = 3 per group). (B) Concentration dependence of the six best siRNAs against CD115 mRNA (n = 3). (C) Experimental design. LPS-treated mice were injected with siRNA against CD115 (siCD115) or control siRNA with an irrelevant sequence (siCON), or left uninjected. (D) CD115 mRNA levels in FACS-isolated monocytes/macrophages (n = 4–6). (E) CD115 expression on monocytes/macrophages by flow cytometry (n = 6–8 per group). (F) Body (n = 3–5) and (G) spleen weight of naive and treated mice (n = 3–10). (H) Total splenocyte count of naive and treated mice (n = 4–9 per group). (I) Serum IFN-γ levels measured by ELISA (n = 3–8). Flow cytometric plots (J) and quantification (K) of monocytes and Ly-6c^{high} monocytes in blood after siRNA treatment (n = 3–5). Data were pooled from 2–5 independent experiments and are mean ± SEM. Significance was determined by Mann-Whitney test or one-way ANOVA. **, P < 0.01; ***, P < 0.001.

The observed lower splenic HSPC retention suggested that M-CSFR knockdown might influence the expression of HSPC retention factors. Indeed, siCD115 treatment significantly reduced mRNA levels of the major retention factors in the bone marrow, including CXCL12, vascular cell adhesion molecule-1 (VCAM-1), angiopoietin, and stem cell factor (SCF; Fig. 3 C). Yet in the spleen, VCAM-1 was the only retention factor significantly reduced by siCD115 treatment (Fig. 3 D). Reducing these retention factors may favor progenitor release into the blood (Winkler et al., 2010). Accordingly, we found that M-CSFR knockdown increased the numbers of circulating LSKs by threefold (Fig. 3 E), indicating increased HSPC departure from their niches in the absence of M-CSFR signaling.

Macrophages' role in the splenic niche

Because M-CSFR regulates macrophage differentiation, survival, and proliferation (Auffray et al., 2009; Hume and MacDonald, 2012), we next enumerated splenic macrophages after silencing this receptor. Treatment with siCD115 substantially reduced the numbers of splenic macrophages (Fig. 4 A). Because macrophages contribute to HSPC maintenance in the bone marrow (Winkler et al., 2010; Chow et al., 2011), we sought to clarify whether and how these cells might regulate the splenic niche. Splenic macrophages express CD169 (Fig. 4 B) and can be efficiently depleted in CD169-iDTR mice (Miyake et al., 2007) via DT treatment (Fig. 4 C). Similar to the effects observed after M-CSFR silencing, this macrophage depletion significantly reduced numbers of splenic HSCs, LSKs, and GMPs (Fig. 4 D). Bone marrow HSC and LSK numbers also fell significantly after macrophage depletion (Fig. 4 E). In contrast, HSCs, LSKs, and GMPs significantly increased in the blood (Fig. 4 F), indicating HSPC mobilization into circulation in the absence of macrophages. Collectively, these data indicate that M-CSFR signaling contributes to the hematopoietic niche by inducing macrophage differentiation.

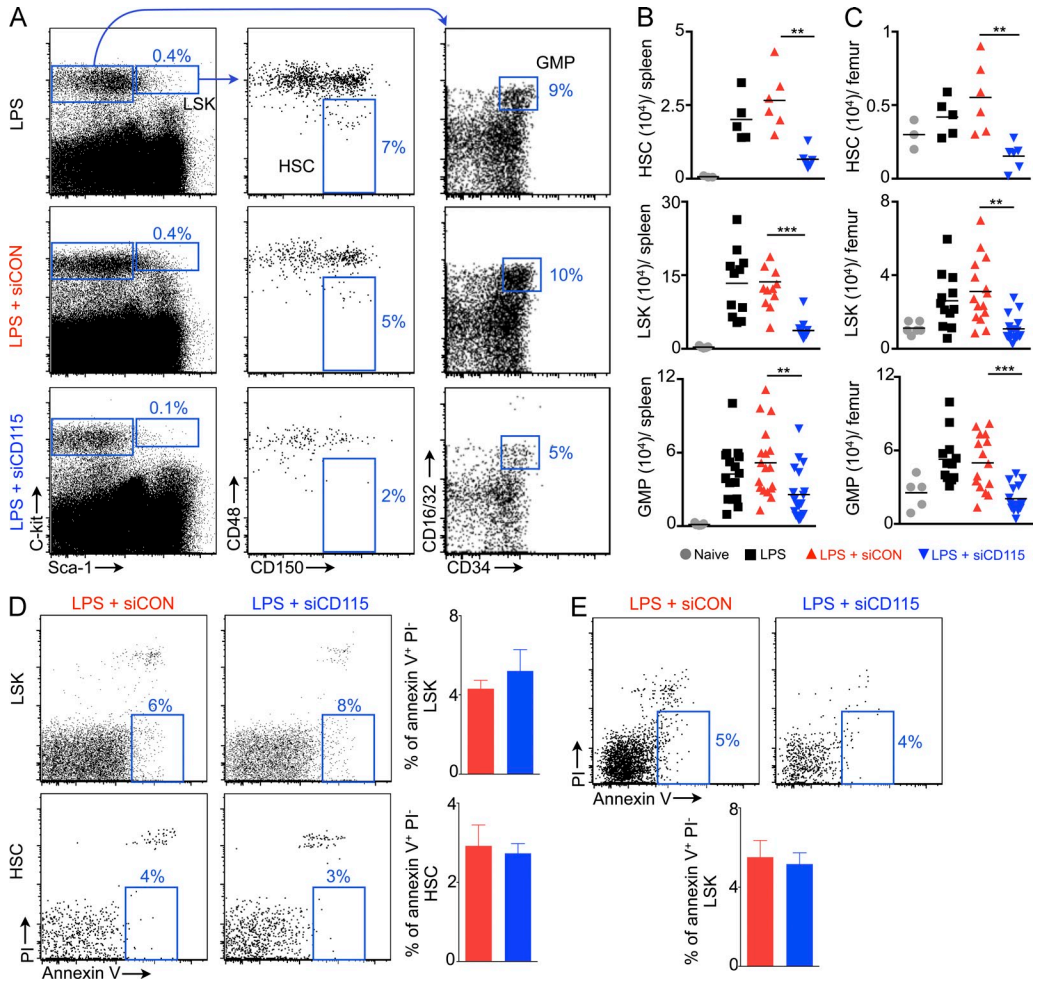

Figure 2. Reduced HSC and progenitor levels in the spleen and bone marrow after CD115 knockdown. (A) Gating for LSKs, HSCs, and GMPs. FACS enumeration of HSCs, LSKs, and GMPs in the spleen (B) and bone marrow (C) after siRNA treatment (n = 3–19). Quantification of apoptotic bone marrow LSKs and HSCs (D) and splenic LSKs (E) after CD115 knockdown (n = 4–5). Data were pooled from 4 (B and C) experiments. (D and E) One of two independent experiments. Data are mean ± SEM. Statistical significance was determined by one-way ANOVA. **, $P < 0.01$; ***, $P < 0.001$.

Splenic resident macrophages retain HSCs via VCAM-1

Because VCAM-1 was the only retention factor that changed in the spleen after M-CSFR knockdown (Fig. 3 D), we investigated which splenocytes express VCAM-1. We found that splenic macrophages (Ulyanova et al., 2005) and endothelial cells express VCAM-1 at high levels (Fig. 5, A and B). We next tested whether splenic HSCs reside close to VCAM-1–expressing cells. Toward this end, we transferred GFP$^+$ HSPCs (LSKs) into LPS-primed mice and imaged splenic sections 3 d later. Transferred GFP$^+$ progenitors localized in numerous splenic locations and formed colonies in the red pulp, indicating their proliferation (Fig. 5 C). GFP$^+$ colonies localized near VCAM-1$^+$ macrophages (Fig. 5 D). Numerous GFP$^+$ cells closely contacted VCAM-1–expressing macrophages in the splenic red pulp (Fig. 5, E and F; and Video 1). Indeed, 44.4 ± 3.7% of GFP$^+$ cells lay in direct contact with or <1 µm distant from VCAM-1$^+$ macrophages (Fig. 5 G). Another 49.4 ± 3.1% of the HSPCs resided within 1–10 µm of VCAM-1$^+$ macrophages.

To investigate if splenic VCAM-1$^+$ macrophages are monocyte-derived or sourced from local progenitors, we induced parabiosis of GFP$^+$ and GFP$^-$ mice (Fig. 5 H). After 6 wk of parabiosis, very few (<1%) VCAM-1$^+$ macrophages were derived from the parabiont, i.e., from circulatory monocytes (Fig. 5, H and I). These data indicate that splenic VCAM-1$^+$ macrophages arise from tissue progenitors rather than the bone marrow, in line with previously published data on splenic macrophages (Yona et al., 2013).

Our data suggest that splenic macrophages retain progenitors via expression of the adhesion molecule VCAM-1. To test this hypothesis directly, we formulated siRNA that targets VCAM-1 within macrophage-avid lipidoid nanoparticles (sense, AcuGGGuuGAcuuucAGGudTsdT; anti-sense, ACCUGAAAGUcAACCcAGUdTsdT). This treatment, which limited VCAM-1 protein concentrations in macrophages but not in endothelial cells (Fig. 6 A), reduced splenic progenitor retention (Fig. 6 B). In contrast, numbers of HSCs, LSKs, and GMPs increased significantly in the circulation (Fig. 6 C),

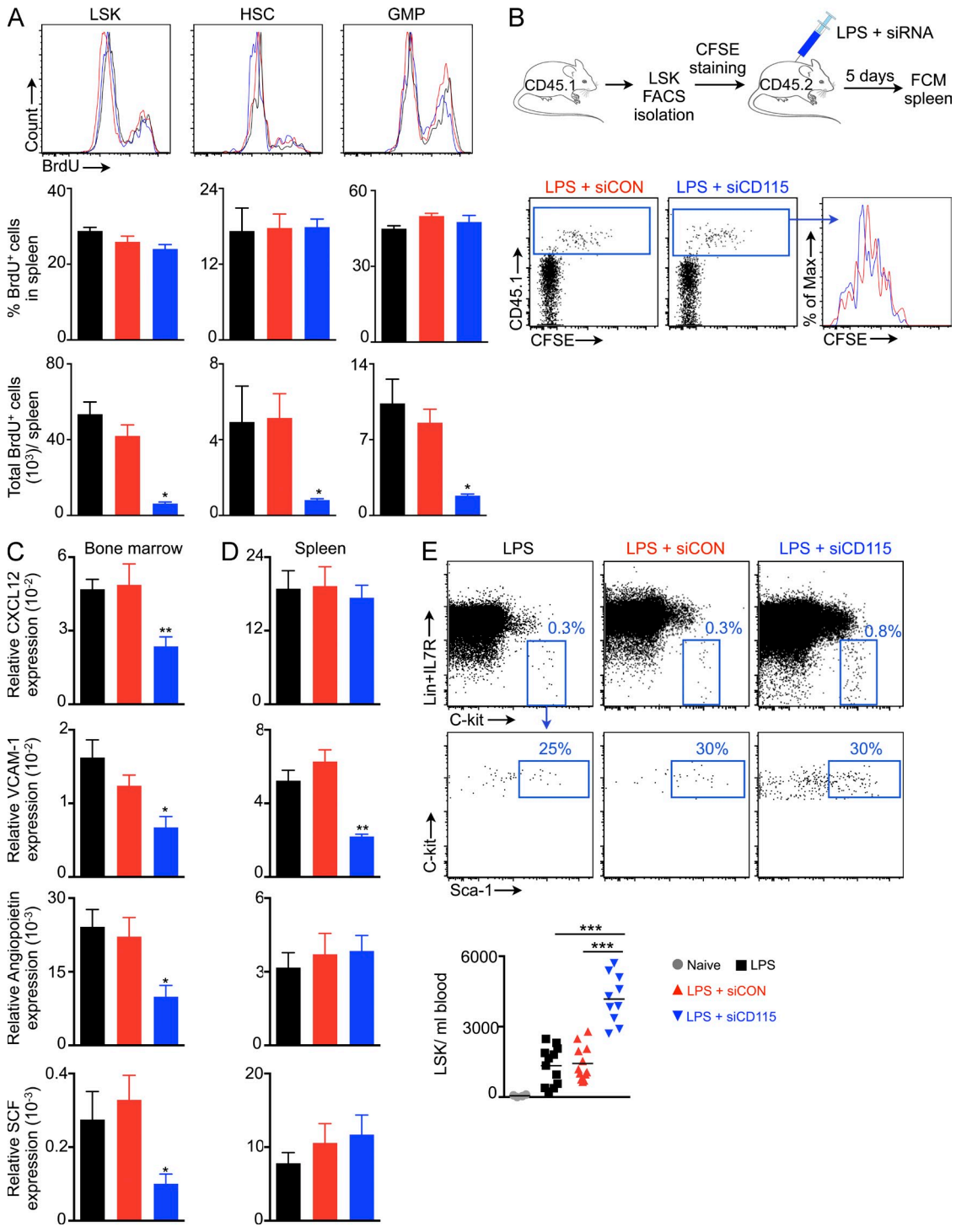

Figure 3. Release of hematopoietic stem and progenitor cells into blood after CD115 knockdown. (A) BrdU+ LSKs, HSCs, and GMPs (top). Quantification of BrdU+ cell % (middle). (bottom) Total BrdU+ LSKs, HSCs, and GMPs in the spleen after siRNA treatment ($n = 3$). (B) CFSE dilution of transferred LSKs ($n = 3$). (C) mRNA levels of HSC retention factors in (C) bone marrow and (D) spleen ($n = 5–6$). (E) LSKs in blood after siRNA treatment ($n = 4–12$). Data were pooled from at least two independent experiments. A and B depict one of two independent experiments. Data are mean ± SEM. Statistical significance was determined by one-way ANOVA. *, $P < 0.05$; **, $P < 0.01$; ***, $P < 0.001$.

indicating mobilization of these cells into the blood after VCAM-1 knockdown in macrophages. In the bone marrow, HSPC numbers did not change significantly after VCAM-1 knockdown in macrophages (Fig. 6 D), pointing to retention mechanisms that compensate for reduced VCAM-1 levels in the bone marrow. Reduced splenic HSC retention may

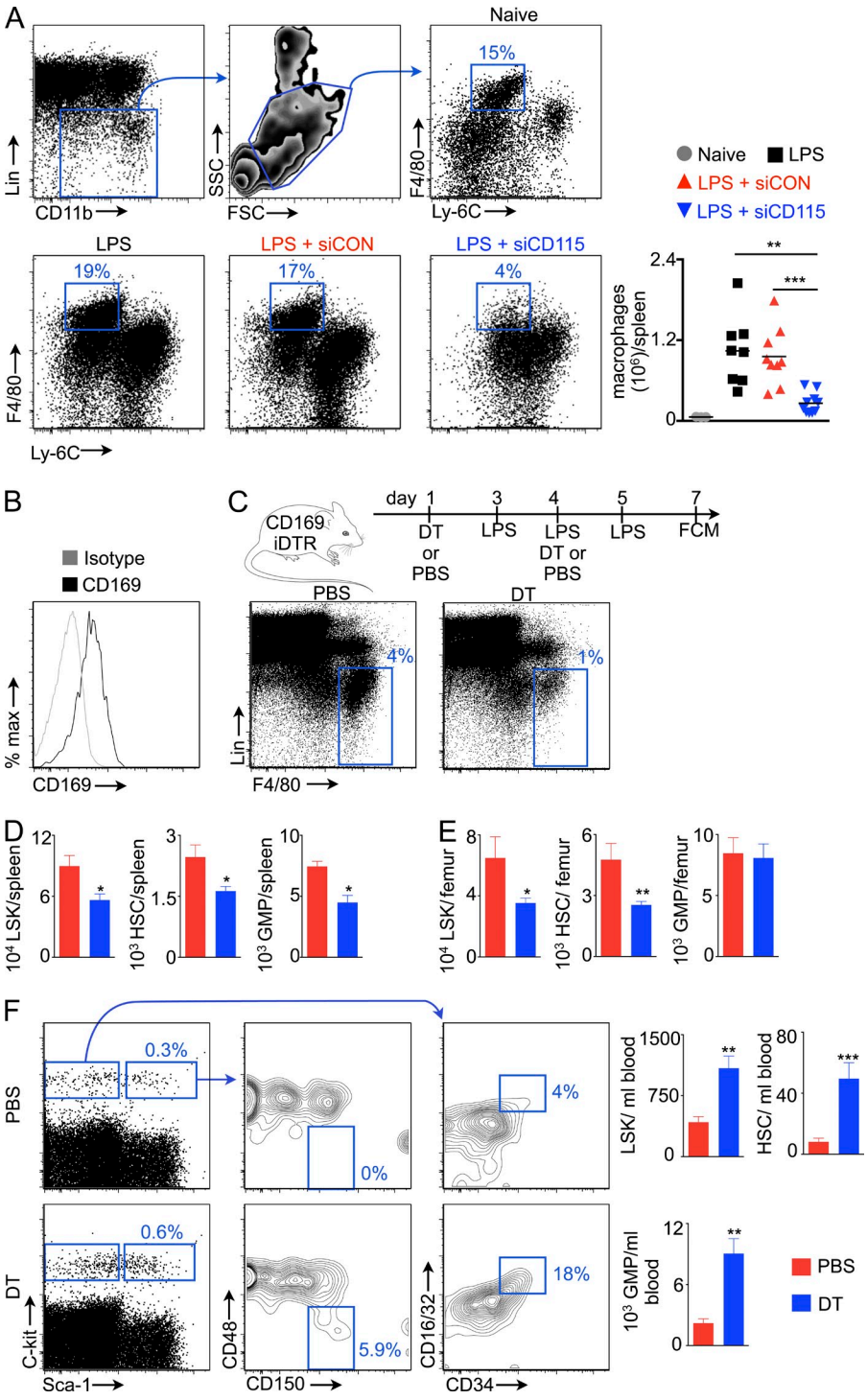

Figure 4. Macrophages maintain splenic HSCs. (A) Gating for splenic macrophages (top). Plots for macrophages in respective groups (bottom; $n = 3–10$). (B) Histogram for CD169 expression on splenic macrophages. (C) Macrophage depletion in CD169 iDTR mice. Plots show depletion of splenic macrophages after diphtheria toxin (DT) treatment. LSKs, HSCs, and GMPs in the spleen (D) and bone marrow (E) of CD169 iDTR mice after depletion ($n = 5–10$). (F) LSKs, HSCs, and GMPs in the blood of PBS and DT-treated mice ($n = 5–9$). Data were pooled from 2–4 independent experiments and are shown as mean ± SEM. Significance was determined by Mann-Whitney test. *, $P < 0.05$; **, $P < 0.01$; ***, $P < 0.001$.

attenuate LPS-induced myelopoiesis. To test this hypothesis, we enumerated myeloid cells and monocytes in the blood (Fig. 6 E) and spleen (Fig. 6 F) and found that VCAM-1 knockdown significantly reduced myeloid cell and monocyte numbers. Collectively, these data demonstrate a requirement for VCAM-1 expression by splenic macrophages for maintaining the organ's hematopoietic niche. VLA-4 is an integrin expressed by leukocytes that binds with VCAM-1 on activated endothelial cells (Elices et al., 1990), resulting in recruitment of inflammatory cells to sites of inflammation. Similarly, VCAM-1 expressed by splenic macrophages may bind with VLA-4 expressed by HSCs (Williams et al., 1991). To investigate an interaction of VCAM-1 with VLA-4 in this setting, we transferred GFP⁺ HSPCs into LPS-treated mice after VLA-4 neutralization

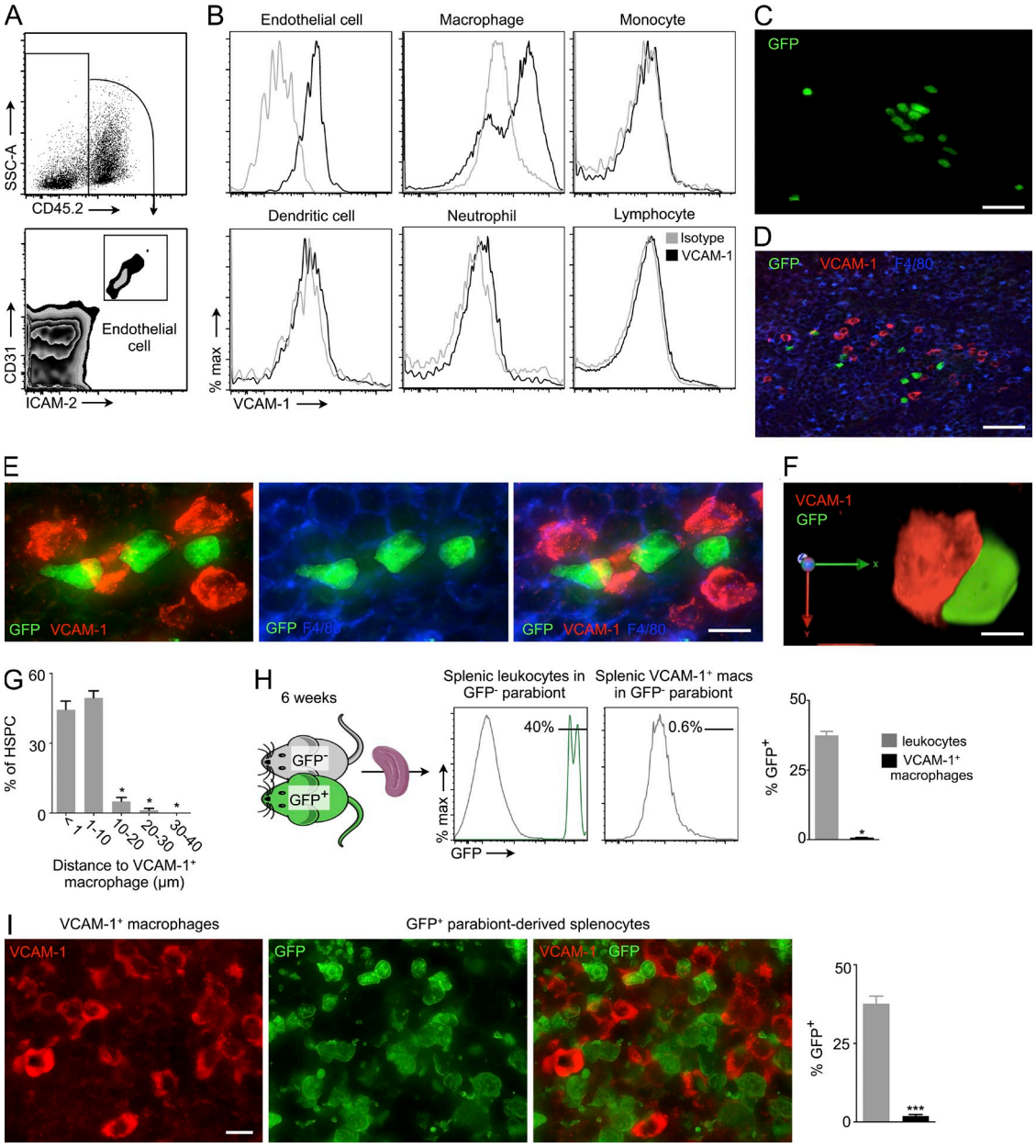

Figure 5. Splenic HSPCs reside near VCAM-1⁺ macrophages. (A) Gating for endothelial cells. CD45.2⁻ CD31^{high} ICAM-2^{high} cells were considered as endothelial cells. (B) VCAM-1 expression on splenic endothelial cell and leukocytes by FACS. (C) Cluster of GFP⁺ cells in the splenic red pulp 3 d after GFP⁺ HSPC transfer into wild-type mouse. Bar, 15 µm. (D) Cluster of GFP⁺ cells (green) near VCAM-1⁺ macrophages (red). Bar, 20 µm. (E) GFP⁺ cells (green) in close contact with VCAM-1⁺ (red) macrophages (F4/80⁺, blue) in the spleen. Bar, 5 µm. (F) 3D image of interaction between a GFP⁺ cell and a VCAM-1⁺ macrophage. (G) Fraction of GFP⁺ cells within indicated distance from VCAM-1⁺ macrophages ($n = 5$). (H) We induced parabiosis of GFP⁺ and GFP⁻ mice. After 6 wk of parabiosis, the spleens of GFP⁻ wild-type mice were analyzed for chimerism (GFP⁺ cells) using flow cytometry (H) and immunofluorescence microscopy (I; $n = 3$). Bar, 10 µm. Data were pooled from two independent experiments. Data are mean ± SEM. Significance was determined by one-way ANOVA and Mann-Whitney test. *, $P < 0.05$; ***, $P < 0.01$.

with an antibody. We found that this blocking antibody significantly decreased splenic HSPC retention (Fig. 6 G).

M-CSFR knockdown reduces inflammation in atherosclerotic plaque

Previous studies revealed that splenic myelopoiesis provides inflammatory monocytes to atherosclerotic plaque (Swirski et al., 2007; Murphy et al., 2011; Robbins et al., 2012) and that, after experimental MI, splenic leukocyte overproduction accelerates progression of atherosclerosis (Dutta et al., 2012). A recent clinical trial indicated that similar mechanisms may exist in humans; ^{18}F-FDG PET/CT showed increased metabolic activity in the spleens of patients with acute coronary syndrome (Kim et al., 2014). We thus investigated

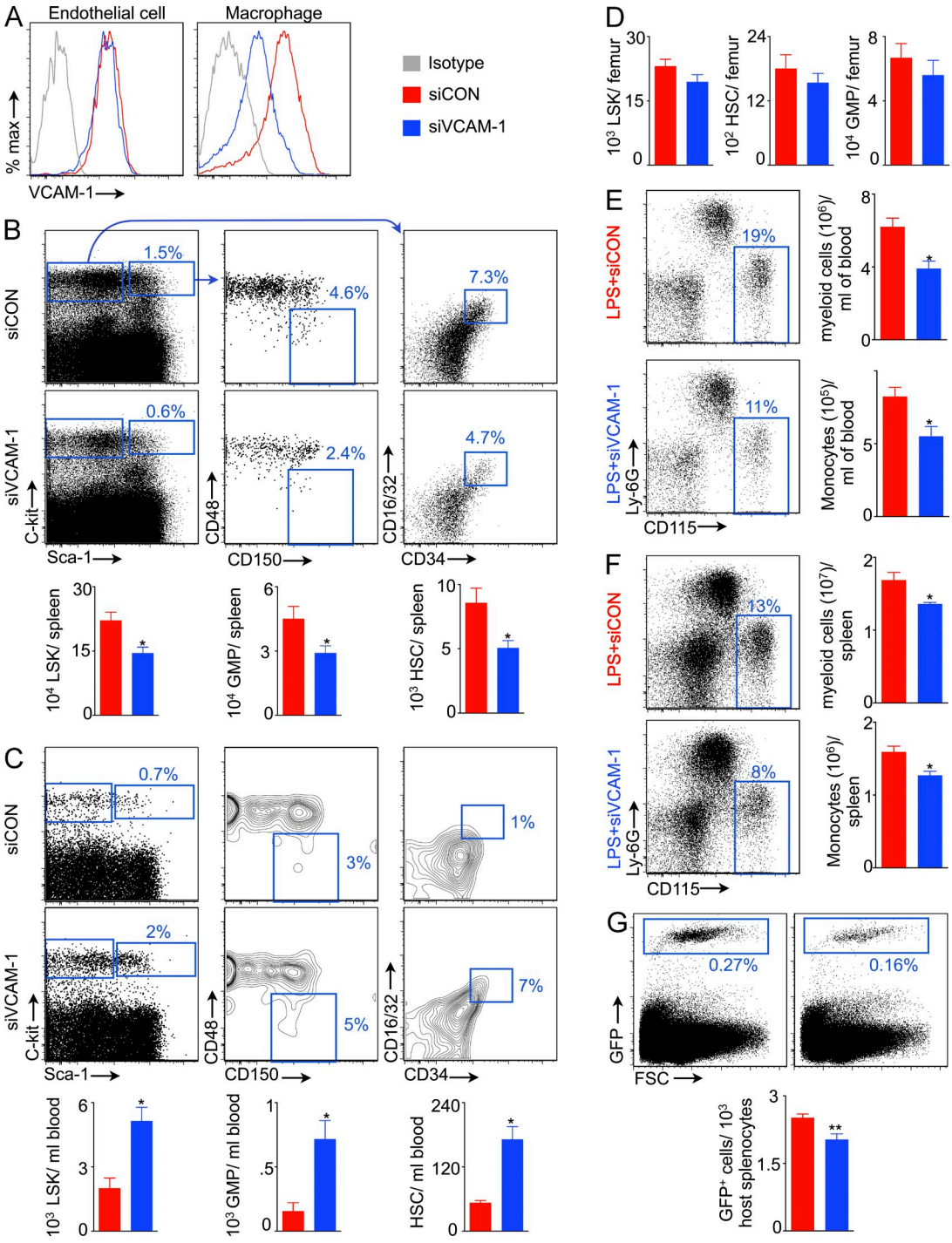

Figure 6. Macrophages retain splenic HSCs via VCAM-1. (A) Flow cytometric plots showing VCAM-1 expression on splenic endothelial cells and macrophages after VCAM-1 knockdown. Flow cytometric plots show percentage of LSKs, HSCs, and GMPs in the spleen (B) and blood (C) of mice treated with siRNA against VCAM-1 (siVCAM-1) or control siRNA (siCON). Levels of LSKs, HSCs, and GMPs in the spleen (B), blood (C), and bone marrow (D; $n = 8–10$). Myeloid cells and monocytes in the blood (E) and spleen (F) after siVCAM-1 treatment in LPS-challenged mice ($n = 4$). (G) Reduced HSPC retention in the spleen after VLA-4 neutralization ($n = 4–5$). Two independent experiments were performed. Data are mean ± SEM. Significance was determined by Mann-Whitney test. *, $P < 0.05$; **, $P < 0.01$.

whether blocking splenic leukocyte overproduction with siCD115, which we found to disrupt the hematopoietic niche, would reduce systemic inflammatory activity in mice with atherosclerosis. *ApoE*$^{-/-}$ mice fed a high fat diet received either siCD115 or siCON, as outlined in Fig. 7 A. In these mice, M-CSFR knockdown reduced splenic HSC and LSK

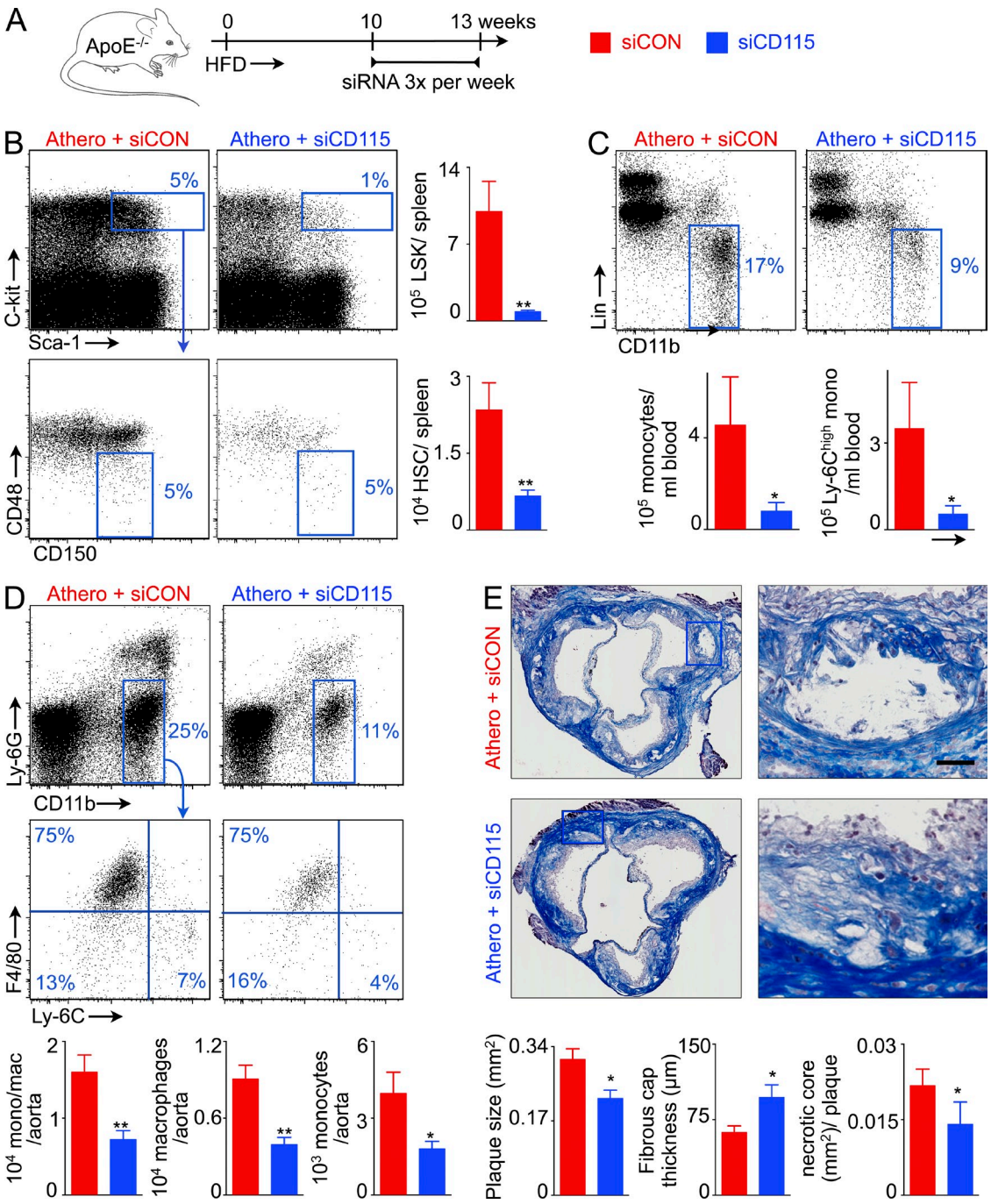

Figure 7. CD115 knockdown reduces inflammation in atherosclerosis. (A) Experimental design. (B) Enumeration of LSKs and HSCs in the spleens of *ApoE*$^{-/-}$ mice after CD115 knockdown. Representative FACS plots show percentage of monocytes in the blood (C), and macrophages and monocytes in the aorta (D) in *ApoE*$^{-/-}$ mice treated with either control or CD115 siRNA. The bar graphs show levels of monocytes and Ly-6c^{high} monocytes in the blood (C) and macrophages and monocytes in the aorta (D) after CD115 knockdown (n = 4–5 per group). (E) Representative images showing Masson staining of the aortic root. The bar graphs depict quantification of total plaque size, fibrous cap thickness, and necrotic core area (n = 5 per group). Experiments were performed in duplicate. Bar, 30 µm. All data are shown as mean ± SEM. Statistical significance was determined by Mann-Whitney test. *, $P < 0.05$; **, $P < 0.01$.

levels by 4- and 12-fold, respectively (Fig. 7 B), leading to much lower blood monocyte counts (Fig. 7 C). In the aorta, siCD115 treatment reduced the numbers of inflammatory myeloid cells, monocytes, and macrophages (Fig. 7 D). In accordance with reduced monocyte accumulation, plaque size, and necrotic core area decreased, and fibrous cap thickness increased in aortic root lesions of siCD115-treated mice (Fig. 7 E).

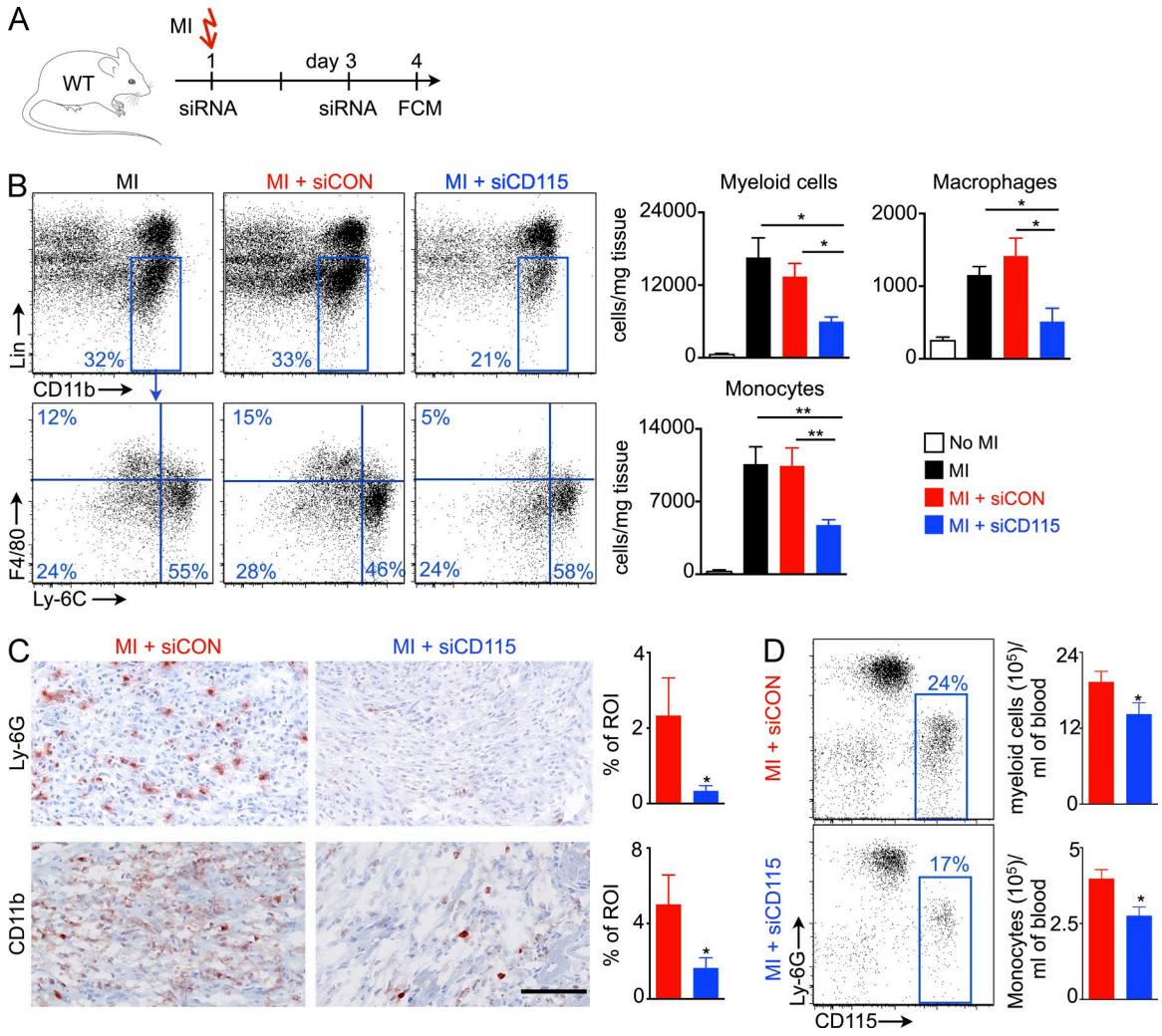

Figure 8. CD115 knockdown reduces inflammation in the infarct after coronary ligation. (A) Experimental design. (B) Myeloid cells, macrophages and monocytes in the infarct (n = 3–7). (C) Histological quantification of Ly-6G and CD11b staining in the infarct (n = 5). Bar, 100 µm. (D) Circulating myeloid cells on day 4 after MI (n = 5). Data were pooled from 3 (B) and 2 (C&D) independent experiments. Data are mean ± SEM. Significance was determined by Mann-Whitney test and one-way ANOVA. *, P < 0.05, **, P < 0.01.

M-CSFR and VCAM-1 knockdown reduces myocardial inflammation after ischemic injury

Coronary occlusion leads to inflammation in the infarcted myocardium (Swirski and Nahrendorf, 2013). To a large extent, infarct macrophages derive from the spleen (Swirski et al., 2009; Leuschner et al., 2012). Leukocyte oversupply or disturbed resolution of inflammation in the heart inhibits the infarct healing process, leading to aggravated left ventricular remodeling and heart failure (Nahrendorf et al., 2007; Panizzi et al., 2010). Although these preclinical observations likely apply to patients after MI (Tsujioka et al., 2009), no therapy targeting post-MI leukocyte oversupply to the heart has improved outcomes to date. We thus investigated whether silencing M-CSFR decreases inflammation in the ischemic heart. To this end, we treated mice with either siCD115 or siCON after coronary ligation (Fig. 8 A). Indeed, siCD115 treatment reduced numbers of myeloid cells, macrophages, and monocytes in the infarcting myocardium 4 d after coronary ligation (Fig. 8 B). Likewise, histologically examined infarct tissue harvested on day 4 after coronary ligation showed significantly reduced Ly-6G and CD11b$^+$ cells after siCD115 treatment (Fig. 8 C). Consistent with this, siCD115-treated mice had lower levels of myeloid cells and monocytes in the blood on day 4 after MI (Fig. 8 D).

Next, we investigated the effect ofVCAM-1 knockdown in macrophages on day 4 after myocardial infarction. siVCAM-1 treatment significantly reduced myeloid cell, monocyte, and macrophage numbers in the infarct (Fig. 9, A and B). Of note, VCAM-1 knockdown did not alter proliferation and apoptosis of infarct macrophages (Fig. 9 C), indicating reduced supply of monocytes after the treatment. Consistent with this notion, we found significantly reduced myeloid cell and monocyte numbers in the blood (Fig. 9 D), bone marrow (Fig. 9 E). and spleen (Fig. 9 F).

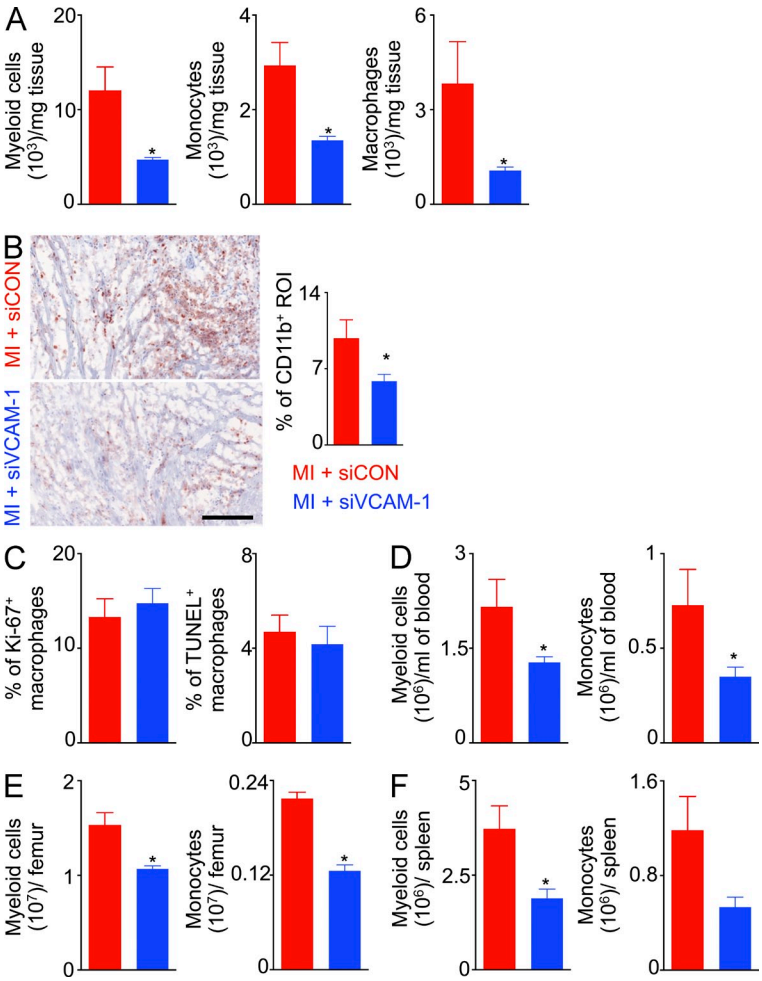

Figure 9. siVCAM-1 treatment reduces inflammation after coronary ligation in C57/Bl6 wild type mice. Lin^- $CD11b^+$ infarct myeloid cells, monocytes and macrophages by flow cytometry (A) and $CD11b^+$ infarct area quantified by immunohistochemistry (B; $n = 4–5$). The scale bar denotes 100 µm. Quantification of proliferating and apoptotic (C) macrophages in the infarct ($n = 4–5$ per group). Lin^-CD11b^+ myeloid cells and monocytes in (D) blood, (E) bone marrow, and (F) spleen ($n = 4–5$). This figure shows data from one of two independent experiments. Data are mean ± SEM. Significance was determined by Mann-Whitney test. *, $P < 0.05$.

VCAM-1 knockdown in macrophages reduces inflammation in atherosclerosis

Because macrophages retain splenic HSCs through VCAM-1, and macrophage-directed VCAM-1 knockdown reduces LPS-induced myelopoiesis (Fig. 6), we hypothesized that VCAM-1 knockdown in macrophages will reduce high fat diet–induced splenic myelopoiesis and decrease inflammation in atherosclerotic plaques. When we treated *ApoE*$^{-/-}$ mice with macrophage-avid nanoparticles delivering siRNA directed at VCAM-1, macrophage and monocyte levels in the aorta fell (Fig. 10 A). To investigate if proliferation and apoptosis of atherosclerotic plaque macrophages depend on VCAM-1, we quantified lesion macrophage proliferation and apoptosis in ApoE$^{-/-}$ mice using flow cytometry after 3 wk of siRNA treatment. We did not find a significant difference in the fraction of macrophages in sub-G0 phase (apoptotic cells) and S–G2–M phase (proliferating cells) between the groups (Fig. 10, B and C). Additionally, we stained aortic root sections for Ki-67 (proliferation) and TUNEL (apoptosis) along with CD68. Immunofluorescence histology confirmed that lesion macrophage apoptosis (Fig. 10 D) and proliferation (Fig. 10 E) do not change after treatment with siVCAM-1. To investigate if macrophage exit is inhibited by VCAM-1, we quantified mRNA levels of macrophage retention and egress cues netrin-1 (van Gils et al., 2012) and CCR7 (Trogan et al., 2006). VCAM-1 knockdown did not significantly change their expression (Fig. 10 F). This treatment reduced LSK and HSC numbers in the spleen (Fig. 10 G), thereby confirming that, in the setting of atherosclerosis, splenic macrophages retain HSCs via VCAM-1. Numbers of Ly-6c^{high} monocytes in the spleen (Fig. 10 H) and blood (Fig. 10 I) fell. VCAM-1 silencing in macrophages significantly decreased plaque size and necrotic cores in the aortic root (Fig. 10 J). However, blood cholesterol levels were unchanged (Fig. 10 K).

DISCUSSION

Patients with myocardial infarction exhibit high leukocyte counts in the blood, inflamed arterial wall, and infarcted myocardium. Exaggerated inflammation in the heart, common in atherosclerotic individuals, promotes left ventricular dilation and heart failure. Extramedullary hematopoiesis, which contributes to leukocyte oversupply at sites of inflammation, occurs in systemic inflammatory conditions such as atherosclerosis (Murphy et al., 2011; Robbins et al., 2012) and after myocardial infarction (Leuschner et al., 2012). Hence, uncovering the pathways leading to extramedullary leukocyte production

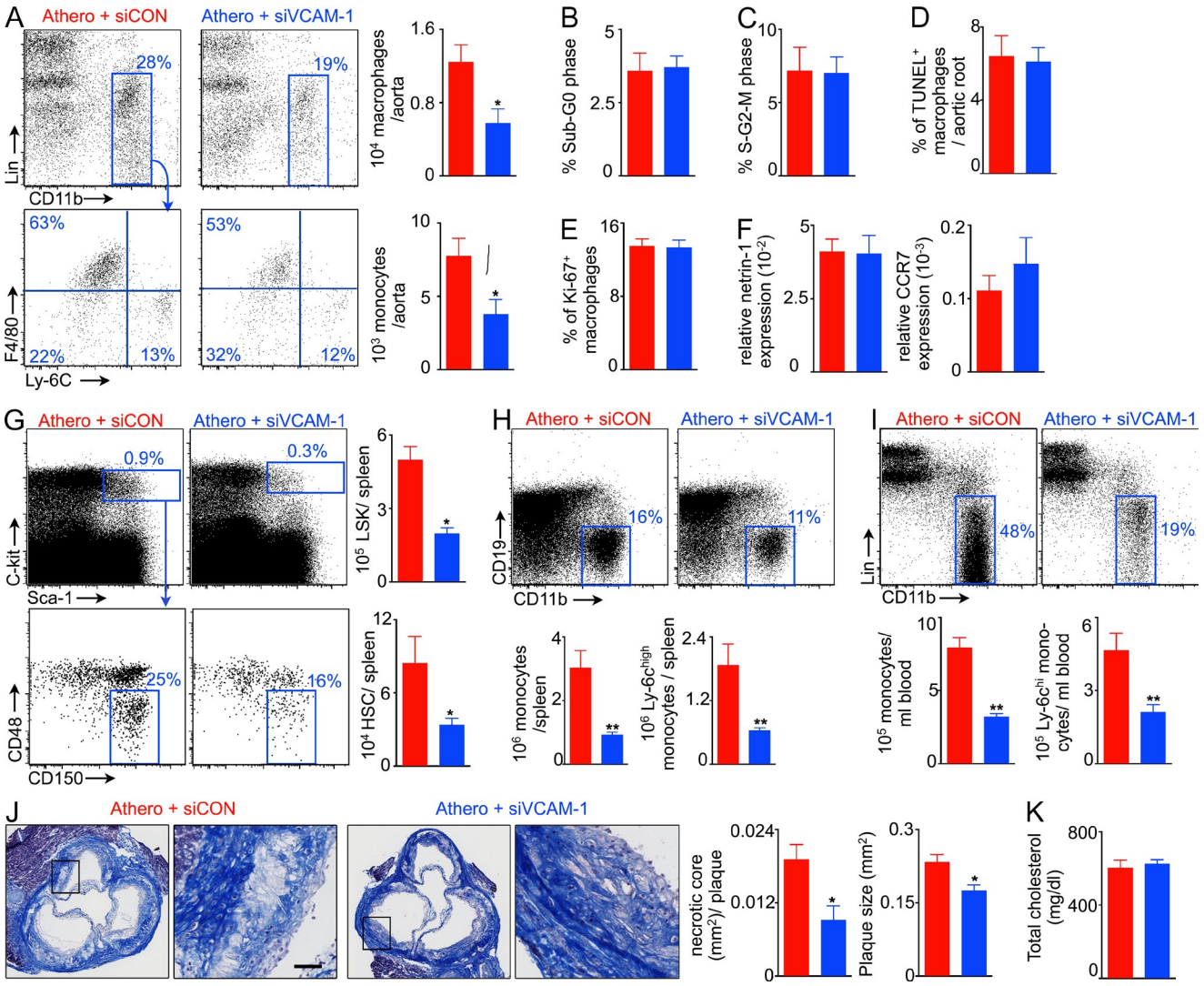

Figure 10. VCAM-1 knockdown in macrophages reduces inflammation in atherosclerosis. *ApoE*$^{-/-}$ mice on high fat diet were injected with control siRNA (siCON) or VCAM-1–targeting siRNA (siVCAM-1) for 3 wk. (A) Macrophages and monocytes in the aorta ($n = 5–6$). Apoptosis and proliferation (B–E) of plaque macrophages by flow cytometry (B and C) and immunofluorescence (D and E; $n = 5$). (F) mRNA of netrin-1 and CCR7 in the aortic root ($n = 4–5$). (G) LSK and HSC levels in the spleen of siCON and siVCAM-1–treated *ApoE*$^{-/-}$ mice ($n = 5$). Monocyte and inflammatory (Ly-6c^{high}) monocyte levels in the spleen (H) and blood (I; $n = 5–6$). (J) Masson staining of the aortic root showing plaque size and necrotic core area ($n = 5$). Bar, 30 µm. (K) Blood cholesterol in ApoE$^{-/-}$ mice ($n = 6$). Data were pooled from at least two experiments and are shown as mean ± SEM. Significance was determined by Mann-Whitney test. *, $P < 0.05$; **, $P < 0.01$.

may reveal therapeutic avenues to mitigate disease-promoting leukocytosis. Although hematopoiesis in the bone marrow has been studied extensively, splenic hematopoiesis remains poorly understood. In the current study, we report that VCAM-1$^+$ macrophages are essential for splenic myelopoiesis and that M-CSFR signaling maintains the spleen's hematopoietic niche. VCAM-1–expressing macrophages retain HSCs in the splenic red pulp, promote extramedullary hematopoiesis, increase systemic levels of inflammatory leukocytes and consequently augment inflammation in atherosclerotic plaques.

Differentiation of monocytes to macrophages depends on M-CSFR signaling (Auffray et al., 2009). Local M-CSF signaling may also regulate tissue-resident macrophage proliferation, as observed, for example, in the growing uterus of a pregnant mouse (Tagliani et al., 2011) and in peritoneal macrophages (Rosas et al., 2014). Moreover, M-CSF improves tissue macrophage survival by reducing apoptosis (Shaposhnik et al., 2010). During atherogenesis, vascular endothelial cells and smooth muscle cells can produce M-CSF (Clinton et al., 1992), and M-CSF–deficient op/op mice have dramatically reduced atherosclerotic plaques (Qiao et al., 1997; Rajavashisth et al., 1998). Our data imply that M-CSF signaling also plays a role in splenic leukocyte production. Because M-CSFR knockdown also affected the bone marrow, our data do not provide information on the relative contribution of the spleen versus bone marrow contribution to the inflammatory response after

MI or LPS challenge, but previous data suggest that the splenic contribution to the infarct myeloid population is substantial (Leuschner et al., 2012). Previous studies showed nanoparticle uptake was highest in macrophages but not strictly limited to these cells; therefore, the described mechanisms may not be exclusive. Because macrophage turnover in atherosclerotic plaque (Robbins et al., 2013) and in acute MI may be rapid (Leuschner et al., 2012), therapeutically targeting the cell's supply by silencing M-CSFR may be a viable way to dampen inflammation in cardiovascular disease. Because human atheromata express M-CSFR, such an intervention might also directly attenuate inflammation at the plaque level (Salomon et al., 1992).

In accordance with mRNA array data on red pulp macrophages, we found these cells express high levels of VCAM-1 and are located in direct proximity to hematopoietic progenitor clusters. HSCs express the VCAM-1 ligand VLA-4 and rely on VCAM-1–VLA-4 interaction to anchor themselves in hematopoietic niches (Williams et al., 1991; Dutta et al., 2012). This type of cell–cell interaction is common in the spleen, which also retains marginal zone B cells (Lu and Cyster, 2002) and innate response activator B cells (Rauch et al., 2012). The latter protect against sepsis via GM-CSF production in the splenic red pulp. Interestingly, GM-CSF expands splenic monocyte production in the setting of atherosclerosis (Robbins et al., 2012; Wang et al., 2014). Our current study reveals that VCAM-1$^+$ red pulp macrophages play a central role in maintaining splenic hematopoiesis.

Early after ischemic injury, increased angiotensin-II concentrations mobilize cells from the splenic monocyte reservoir, which contributes ~50% of leukocytes to the infarct. Later, the spleen continues to supply myeloid cells to the ischemic as well as the remote myocardium, now relying on IL-1β and SCF signaling to enhance splenic monocyte production (Dutta et al., 2012). Hematopoietic activity in the spleen follows the recruitment of bone marrow HSPCs, which circulate in higher numbers after MI in mice (Dutta et al., 2012) and in patients (Massa et al., 2005; Assmus et al., 2012). The relocation of HSPCs from the murine bone marrow to the spleen accelerates production of inflammatory myeloid cells, exacerbating preexisting atherosclerosis (Dutta et al., 2012). HSPC retention in hematopoietic tissue in the bone marrow and the spleen (Williams et al., 1991; Scott et al., 2003; Dutta et al., 2012) relies at least partially on the integrin VLA-4, a ligand for VCAM-1, which we report to be expressed by splenic macrophages. Even without an acute inflammatory trigger, such as MI, splenic myelopoiesis occurs in mice with chronic atherosclerosis (Robbins et al., 2012). In *ApoE*$^{-/-}$ mice on a high fat diet, HSPCs differentiate into monocytes in the spleen, a process that depends on GM-CSF and IL-3 (Wang et al., 2014). These monocytes then enter the circulation and migrate to atherosclerotic plaques. In the vessel wall, the cells and their progeny secrete inflammatory cytokines, give rise to reactive oxygen species, and produce proteases, all of which may render atherosclerotic plaques vulnerable to rupture (Moore and Tabas, 2011).

Despite growing evidence of the importance of inflammation in atherosclerosis and heart failure, specific antiinflammatory therapy has yet to be implemented in the clinic. Ongoing trials explore whether antiinflammatory therapeutics, such as anti-IL1β–neutralizing antibodies (CANTOS, NCT01327846) and methotrexate (CIRT, NCT01594333) reduce ischemic complications and death in patients with atherosclerosis. In addition to biologicals or small molecule drugs, RNAi may therapeutically interfere with the life cycles of inflammatory leukocytes that drive atherosclerosis progression and complication. Recent progress in RNAi delivery has led to clinical trials (Coelho et al., 2013) and enabled leukocyte silencing in rodents and primates (Novobrantseva et al., 2012). The 70-nm particles used in the current study of siRNA delivery to macrophages were identified in large-scale screens (Love et al., 2010), are rapidly synthesized from four components, and are similar to safe materials advancing through clinical trials. Our data indicate that RNAi targeting of hematopoiesis could reduce systemic inflammation by curtailing leukocyte overproduction. Silencing M-CSFR expression disrupted the splenic hematopoietic niche assembly, potentially allowing for decisive antiinflammatory intervention in individuals with vulnerable plaques or shortly after myocardial infarction. Currently, this approach would lend itself to short-term, systemic, parenteral delivery rather than sustained oral therapy. Longer therapeutic courses might compromise the salutary functions of M-CSF signaling and macrophages in host defenses. Because the siRNA delivery in our study was systemic and therefore not limited to splenic cells, we are unable to define to what precise degree the observed therapeutic effects derive from silencing in the spleen. Likely, monocyte differentiation in the bone marrow or at the sites of inflammation, i.e., the heart and the arterial wall, also contributed to lower macrophage numbers. Yet, the parallel and profound reduction of monocytes in the circulation and inflamed tissue indicates that lowering the systemic supply of inflammatory cells played a major role in reducing inflammation in the target tissue.

In conclusion, this study identifies a novel role for signaling through the M-CSFR in the genesis of splenic myelopoiesis. Interfering with this receptor inhibits macrophage functions in the splenic hematopoietic niche. These cells express VCAM-1 to retain HSPCs in the splenic red pulp. Interrupting this pathway with myeloid-directed in vivo RNAi, by silencing either M-CSFR or VCAM-1, enables HSPCs to escape from niches into blood and substantially reduces circulating monocytes. Ours is a first study on how RNAi affects hematopoiesis. Finally, this intervention decreases inflammatory cell numbers in atherosclerotic plaque and in the ischemic myocardium, illustrating an innovative approach to treating patients with atherosclerosis.

MATERIALS AND METHODS

Animal strains and surgical procedures. C57BL/6J, B6. SJL-Ptprc^a Pepc^b/BoyJ (CD45.1), and B6.129P2-*Apoe*^{tm1Unc}/J (*ApoE*$^{-/-}$) mice were purchased from The Jackson Laboratory. ApoE$^{-/-}$ mice consumed a

high-cholesterol diet (Harlan Teklad; 0.2% total cholesterol) for 10 wk before the experiments. CD169-iDTR mice were gifts from M. Tanaka (Institute of Physical and Chemical Research Center for Allergy and Immunology, Yokohama, Japan). CD169-iDTR litter mates were used as control. For other strains, appropriate control mice were purchased from Jackson Laboratory. All animal experiments were approved by Massachusetts General Hospital's Institutional Animal Care and Use Committee.

To induce myocardial infarction, mice were intubated and ventilated with 2% isoflurane, and then underwent thoracotomy in the fourth left intercostal space. The left coronary artery was permanently ligated with a monofilament nylon 8–0 suture. The thorax was closed with a 5–0 suture.

siRNA formulation and in-vitro screening. siRNAs duplexes were generated to target the CSFR1 (M-CSFR) transcript. Single-strand RNAs were designed and produced at Alnylam Pharmaceuticals as described previously (Frank-Kamenetsky et al., 2008). The NIH 3T3 cell line was transfected with siRNAs targeting M-CSFR or nontargeting control siRNA complexed with Lipofectamine RNAiMAX Transfection Reagent (Invitrogen) at 0.5 and 5 nM final concentrations. Cells were harvested 24 h after transfection, and expression levels of M-CSFR mRNA were quantified by the branched DNA QuantiGene 2.0 assay (Affymetrix) using mouse M-CSFR–specific probes. Dose response was performed on the best siRNA duplexes with an siRNA, with the best siRNA having an EC_{50} of 10 pM. This M-CSFR–targeted siRNA (siCD115) was scaled up for in vivo studies and has the following sequence: cuAcucAAcuuucuccGAAdTsdT (sense), UUCGGAGAAAGUUGAGuAGdTsdT antisense), wherein lower case letters identify 2′OMe modified nucleotides. VCAM-1–targeting siRNA was identified similarly, except C2C12 cells were used for siRNA screening and qRT-PCR using TaqMan primers, and probes were mRNA quantification. The VCAM-1–specific duplex selected for in vivo studies has the following sequence: AcuGGGuuGAcuuucAGGudTsdT (sense), ACCUGAAAGUcAACCcAGUdTsdT (antisense). M-CSFR and VCAM1 targeting siRNAs were independently encapsulated into nanoparticle formulations as described previously (Akinc et al., 2008; Leuschner et al., 2011).

Treatment protocol. C57BL/6 mice were treated with 10 µg of LPS for three consecutive days before tissue harvesting on the fourth day. siRNA against either M-CSFR or VCAM-1 was administered i.v. at 0.5 mg/kg body weight on the first and third day. To test efficacy of the siRNA after myocardial infarction, siRNA against either M-CSFR or VCAM-1 was injected i.v. at 0.5 mg/kg body weight on the day of MI and 2 d after MI. *ApoE*$^{-/-}$ mice were injected with the siRNA three times per week for 3 wk. CD169-iDTR mice were injected with DT i.v. at 10 µg/kg body weight on the first and fourth days before analysis on the seventh day.

Organ harvesting and tissue processing. Cardiac puncture was performed to draw blood with an insulin syringe in 50 mM EDTA (Sigma-Aldrich). Red blood cell lysis was performed with 1× RBC lysis buffer (BioLegend) according to the manufacturer's protocol. Hearts were minced and digested in 450 U/ml collagenase I, 125 U/ml collagenase XI, 60 U/ml DNase I, and 60 U/ml hyaluronidase (Sigma-Aldrich) at 37°C at 750 rpm for 1 h. Cells were washed in 10 ml FACS buffer (PBS with 0.5% bovine serum albumin and 1% fetal bovine serum) and filtered through 40-µm mesh to obtain single-cell suspension. Spleens were minced in FACS buffer and passed through 40-µm filters, followed by red blood cell lysis in the filtrate. Femurs were flushed with ice-cold FACS buffer.

Flow cytometry. Single cell suspensions (300 µl in FACS buffer) were stained with a cocktail of antibodies against lineage markers (CD90 [clone 53–2.1], B220 [clone RA3-6B2], CD49b [clone DX5], NK1.1 [clone PK136], Ly-6G [clone 1A8], and Ter-119 [clone TER-119]). After 30 min of staining, the cells were washed in FACS buffer and stained with antibodies against leukocyte markers (CD11b (clone M1/70), CD11c (clone HL3), F4/80 (clone BM8), and Ly6C (clone AL-21)).

For hematopoietic stem and progenitor cell staining, we used biotin-conjugated antibodies against lineage markers CD11b (clone M1/70), CD11c (clone N418), and IL7Rα (clone A7R34) in addition to the lineage antibodies used for leukocyte staining. This was followed by a secondary staining with antibodies against c-Kit (clone 2B8), Sca-1 (clone D7), CD16/32 (clone 2.4G2), CD34 (clone RAM34), CD115 (clone AFS98), CD150 (9D1), and CD48 (HM48-1).

HSC proliferation assays. Mice were injected with BrdU 24 h before organ collection, and intracellular BrdU staining was performed using BrdU flow kits (BD). For CFSE dilution assay, sorted LSKs were stained with CFSE (Invitrogen) according to manufacturer's protocol and injected into B6 mice treated with LPS and either siCON or siCD115. BrdU incorporation and CFSE dilution in hematopoietic stem and progenitor cells were measured by an LSRII.

HSC apoptosis assay. 5,000,000 bone marrow cells or splenocytes were cultured in 1 ml of DMEM and camptothecin (20 µM) for 3 h to induce apoptosis. Apoptotic HSCs were stained with Annexin V/dead cell apoptosis kit (Invitrogen) and quantified by flow cytometry.

VLA-4 neutralization. Mice were injected i.v. with 200 µg of either anti–mouse VLA-4 (BioXCell) or control rat IgG2b (BioXCell) 2 d after LPS injection. About 300,000 lineage$^-$ c-kit$^+$ Sca-1$^+$ cells sorted from GFP$^+$ mice were adoptively transferred i.v. on the day of VLA-4 injection.

Total blood cholesterol measurement and ELISA. Blood was collected via cardiac puncture in Eppendorf tubes without anticoagulant. Blood was kept at room temperature for ∼2 h and spun down at 4°C for 10 min to separate serum. Serum was stored at −80°C, and total cholesterol was measured using an enzymatic colorimetric assay (Cholesterol E; Wako). We used Quantikine Colorimetric Sandwich ELISA kit (R&D Systems) to measure serum IFN-γ levels.

FACS. Bones were harvested, including all long bones and the spine. Single-cell suspensions were prepared by grinding bones with a pestle and mortar and passing the cells through 40-µm filters. The cells were stained with biotinylated antibodies against lineage markers for hematopoietic stem and progenitor cells, as described above, and then incubated with streptavidin MicroBeads (Miltenyi Biotec). Lineage$^+$ cells were depleted using MACS columns (Miltenyi Biotec). Lin$^-$ cells were stained with antibodies for hematopoietic stem and progenitor cells as described above. LSKs were sorted using a FACSAria IIu cell sorter (BD).

RNA extraction and quantification. RNA was extracted using PicoPure RNA isolation kit (Applied Biosystems) and eluted in a total volume of 10 µl. RNA was quantified using Nanodrop, and one microgram of mRNA was used to generate complimentary DNA (cDNA) using a high capacity RNA to cDNA kit (Applied Biosystems). Target genes were quantified using TaqMan gene expression assays (Applied Biosystems).

Histology. For histological analysis, aortas and hearts were embedded in OCT compound (Sakura Finetek), and fresh-frozen serial 6 µm thick sections were prepared. Masson Trichrome staining was performed according to the manufacturer's instructions (Sigma-Aldrich) to assess plaque size, fibrous cap thickness and necrotic core. Immunohistochemistry was performed using Ly-6G (1A8, BioLegend) and CD11b (M1/70, BD) antibodies, biotinylated anti-rat IgG antibody (Vector Laboratories Inc.) and VECTASTAIN ABC kit (Vector Laboratories). The reaction was visualized using a 3-amino-9-ethylcarbazole (AEC) substrate (Dako), and all sections were counterstained with Harris hematoxylin solution (Sigma-Aldrich). The slides were scanned using Nanozoomer 2.0RS (Hamamatsu), and staining was quantified in 5 high power fields per mouse, using semiautomated thresholding in IPLab, and expressed as percentage of positive area.

Immunofluorescence microcopy. 3 d after priming with LPS, the spleen was harvested and fixed by immersion in a 4% PFA PBS solution. Fixed tissues were cryoprotected in a 30% sucrose, 0.02% sodium azide, PBS solution at 4°C. Tissues were embedded and frozen in tissue freezing media (Leica) and then sectioned in a −20°C cryostat (Leica) at a thickness of 10 and 25 µm.

The tissue sections were stained with an anti–VCAM-1 antibody (sc-1504; Santa Cruz Biotechnology) and an anti-F4/80 (14–4801; eBioscience) antibody followed by a Cy3 donkey anti–rabbit and Cy5 donkey anti–rat IgG (Jackson ImmunoResearch Laboratories). Sections were mounted in Vectashield + DAPI mounting media.

Microscopic images were acquired with an Eclipse 90i epifluorescence microscope (Nikon). Digital image files were post-processed with Nikon Imaging Software Elements, Volocity 6 (Perkin Elmer), ImageJ, and IP laboratory.

For Ki-67 immunofluorescence imaging, heart tissue sections were stained with FITC Ki-67 (clone SP6, dilution 1:25; Abcam). To detect apoptotic cardiac macrophages, TUNEL reagents (DeadEnd Fluorometric TUNEL System; Promega) were used according to the manufacturer's protocol.

Online supplemental material. Video 1 shows interaction between HSPCs and VCAM-1$^+$ macrophages in the spleen. Online supplemental material is available at http://www.jem.org/cgi/content/full/jem.20141642/DC1.

We thank Dr. Masato Tanaka (Institute of Physical and Chemical Research Center for Allergy and Immunology, Yokohama, Kanagawa, Japan) for providing CD169-DTR mice and the Alnylam siRNA synthesis and formulations groups for siRNA synthesis and encapsulation.

This work was funded in part by grants from the National Institutes of Health R01-HL114477, R01-HL117829, R01-NS084863 (M. Nahrendorf), HHSN268201000044C (R. Weissleder), K99-HL121076 (P. Dutta), and R01-HD069623 (N. Da Silva). H.B. Sager is funded by Deutsche Forschungsgemeinschaft (SA1668/2-1).

T. Novobrantseva, V.M. Ruda, A. Borodovsky, and K. Fitzgerald are current or former employees of Alnylam Pharmaceuticals. The authors have no additional financial interests.

Submitted: 25 August 2014
Accepted: 13 February 2015

REFERENCES

Akinc, A., A. Zumbuehl, M. Goldberg, E.S. Leshchiner, V. Busini, N. Hossain, S.A. Bacallado, D.N. Nguyen, J. Fuller, R. Alvarez, et al. 2008. A combinatorial library of lipid-like materials for delivery of RNAi therapeutics. *Nat. Biotechnol.* 26:561–569. http://dx.doi.org/10.1038/nbt1402

Assmus, B., M. Iwasaki, V. Schächinger, T. Roexe, M. Koyanagi, K. Iekushi, Q. Xu, T. Tonn, E. Seifried, S. Liebner, et al. 2012. Acute myocardial infarction activates progenitor cells and increases Wnt signalling in the bone marrow. *Eur. Heart J.* 33:1911–1919. http://dx.doi.org/10.1093/eurheartj/ehr388

Auffray, C., M.H. Sieweke, and F. Geissmann. 2009. Blood monocytes: development, heterogeneity, and relationship with dendritic cells. *Annu. Rev. Immunol.* 27:669–692. http://dx.doi.org/10.1146/annurev.immunol.021908.132557

Chow, A., D. Lucas, A. Hidalgo, S. Méndez-Ferrer, D. Hashimoto, C. Scheiermann, M. Battista, M. Leboeuf, C. Prophete, N. van Rooijen, et al. 2011. Bone marrow CD169+ macrophages promote the retention of hematopoietic stem and progenitor cells in the mesenchymal stem cell niche. *J. Exp. Med.* 208:261–271. http://dx.doi.org/10.1084/jem20101688

Clinton, S.K., R. Underwood, L. Hayes, M.L. Sherman, D.W. Kufe, and P. Libby. 1992. Macrophage colony-stimulating factor gene expression in vascular cells and in experimental and human atherosclerosis. *Am. J. Pathol.* 140:301–316.

Coelho, T., D. Adams, A. Silva, P. Lozeron, P.N. Hawkins, T. Mant, J. Perez, J. Chiesa, S. Warrington, E. Tranter, et al. 2013. Safety and efficacy of RNAi therapy for transthyretin amyloidosis. *N. Engl. J. Med.* 369:819–829. http://dx.doi.org/10.1056/NEJMoa1208760

Courties, G., T. Heidt, M. Sebas, Y. Iwamoto, D. Jeon, J. Truelove, B. Tricot, G. Wojtkiewicz, P. Dutta, H.B. Sager, et al. 2014. In vivo silencing of the transcription factor IRF5 reprograms the macrophage phenotype and improves infarct healing. *J. Am. Coll. Cardiol.* 63:1556–1566.

Dahlman, J.E., C. Barnes, O.F. Khan, A. Thiriot, S. Jhunjunwala, T.E. Shaw, Y. Xing, H.B. Sager, G. Sahay, L. Speciner, et al. 2014. In vivo endothelial siRNA delivery using polymeric nanoparticles with low molecular weight. *Nat. Nanotechnol.* 9:648–655. http://dx.doi.org/10.1038/nnano.2014.84

Dai, X.M., G.R. Ryan, A.J. Hapel, M.G. Dominguez, R.G. Russell, S. Kapp, V. Sylvestre, and E.R. Stanley. 2002. Targeted disruption of the mouse colony-stimulating factor 1 receptor gene results in osteopetrosis, mononuclear phagocyte deficiency, increased primitive progenitor cell frequencies, and reproductive defects. *Blood.* 99:111–120. http://dx.doi.org/10.1182/blood.V99.1.111

Ding, L., and S.J. Morrison. 2013. Haematopoietic stem cells and early lymphoid progenitors occupy distinct bone marrow niches. *Nature.* 495:231–235. http://dx.doi.org/10.1038/nature11885

Ding, L., T.L. Saunders, G. Enikolopov, and S.J. Morrison. 2012. Endothelial and perivascular cells maintain haematopoietic stem cells. *Nature.* 481:457–462. http://dx.doi.org/10.1038/nature10783

Dutta, P., G. Courties, Y. Wei, F. Leuschner, R. Gorbatov, C.S. Robbins, Y. Iwamoto, B. Thompson, A.L. Carlson, T. Heidt, et al. 2012. Myocardial infarction accelerates atherosclerosis. *Nature.* 487:325–329. http://dx.doi.org/10.1038/nature11260

Elices, M.J., L. Osborn, Y. Takada, C. Crouse, S. Luhowskyj, M.E. Hemler, and R.R. Lobb. 1990. VCAM-1 on activated endothelium interacts with the leukocyte integrin VLA-4 at a site distinct from the VLA-4/fibronectin binding site. *Cell.* 60:577–584. http://dx.doi.org/10.1016/0092-8674(90)90661-W

Frank-Kamenetsky, M., A. Grefhorst, N.N. Anderson, T.S. Racie, B. Bramlage, A. Akinc, D. Butler, K. Charisse, R. Dorkin, Y. Fan, et al. 2008. Therapeutic RNAi targeting PCSK9 acutely lowers plasma cholesterol in rodents and LDL cholesterol in nonhuman primates. *Proc. Natl. Acad. Sci. USA.* 105:11915–11920. http://dx.doi.org/10.1073/pnas.0805434105

Hume, D.A., and K.P. MacDonald. 2012. Therapeutic applications of macrophage colony-stimulating factor-1 (CSF-1) and antagonists of CSF-1 receptor (CSF-1R) signaling. *Blood.* 119:1810–1820. http://dx.doi.org/10.1182/blood-2011-09-379214

Kiel, M.J., O.H. Yilmaz, T. Iwashita, O.H. Yilmaz, C. Terhorst, and S.J. Morrison. 2005. SLAM family receptors distinguish hematopoietic stem and progenitor cells and reveal endothelial niches for stem cells. *Cell.* 121:1109–1121. http://dx.doi.org/10.1016/j.cell.2005.05.026

Kim, E.J., S. Kim, H.S. Seo, and D.O. Kang. 2014. The Metabolic Activity of the Spleen and Bone Marrow in Patients with Acute Myocardial Infarction Evaluated by 18F-FDG PET Imaging. *Circ Cardiovasc Imaging.* http://dx.doi.org/10.1161/CIRCIMAGING.113.001093

Leuschner, F., P. Dutta, R. Gorbatov, T.I. Novobrantseva, J.S. Donahoe, G. Courties, K.M. Lee, J.I. Kim, J.F. Markmann, B. Marinelli, et al. 2011. Therapeutic siRNA silencing in inflammatory monocytes in mice. *Nat. Biotechnol.* 29:1005–1010. http://dx.doi.org/10.1038/nbt.1989

Leuschner, F., P.J. Rauch, T. Ueno, R. Gorbatov, B. Marinelli, W.W. Lee, P. Dutta, Y. Wei, C. Robbins, Y. Iwamoto, et al. 2012. Rapid monocyte kinetics in acute myocardial infarction are sustained by extramedullary monocytopoiesis. *J. Exp. Med.* 209:123–137. http://dx.doi.org/10.1084/jem.20111009

Love, K.T., K.P. Mahon, C.G. Levins, K.A. Whitehead, W. Querbes, J.R. Dorkin, J. Qin, W. Cantley, L.L. Qin, T. Racie, et al. 2010. Lipid-like materials for low-dose, in vivo gene silencing. *Proc. Natl. Acad. Sci. USA.* 107:1864–1869. http://dx.doi.org/10.1073/pnas.0910603106

Lu, T.T., and J.G. Cyster. 2002. Integrin-mediated long-term B cell retention in the splenic marginal zone. *Science.* 297:409–412. http://dx.doi.org/10.1126/science.1071632

Majmudar, M.D., E.J. Keliher, T. Heidt, F. Leuschner, J. Truelove, B.F. Sena, R. Gorbatov, Y. Iwamoto, P. Dutta, G. Wojtkiewicz, et al. 2013. Monocyte-directed RNAi targeting CCR2 improves infarct healing in atherosclerosis-prone mice. *Circulation.* 127:2038–2046. http://dx.doi.org/10.1161/CIRCULATIONAHA.112.000116

Massa, M., V. Rosti, M. Ferrario, R. Campanelli, I. Ramajoli, R. Rosso, G.M. De Ferrari, M. Ferlini, L. Goffredo, A. Bertoletti, et al. 2005. Increased circulating hematopoietic and endothelial progenitor cells in the early phase of acute myocardial infarction. *Blood*. 105:199–206. http://dx.doi.org/10.1182/blood-2004-05-1831

Miyake, Y., K. Asano, H. Kaise, M. Uemura, M. Nakayama, and M. Tanaka. 2007. Critical role of macrophages in the marginal zone in the suppression of immune responses to apoptotic cell-associated antigens. *J. Clin. Invest.* 117:2268–2278. http://dx.doi.org/10.1172/JCI31990

Moore, K.J., and I. Tabas. 2011. Macrophages in the pathogenesis of atherosclerosis. *Cell*. 145:341–355. http://dx.doi.org/10.1016/j.cell.2011.04.005

Murphy, A.J., M. Akhtari, S. Tolani, T. Pagler, N. Bijl, C.L. Kuo, M. Wang, M. Sanson, S. Abramowicz, C. Welch, et al. 2011. ApoE regulates hematopoietic stem cell proliferation, monocytosis, and monocyte accumulation in atherosclerotic lesions in mice. *J. Clin. Invest.* 121:4138–4149. http://dx.doi.org/10.1172/JCI57559

Nahrendorf, M., F.K. Swirski, E. Aikawa, L. Stangenberg, T. Wurdinger, J.L. Figueiredo, P. Libby, R. Weissleder, and M.J. Pittet. 2007. The healing myocardium sequentially mobilizes two monocyte subsets with divergent and complementary functions. *J. Exp. Med.* 204:3037–3047. http://dx.doi.org/10.1084/jem.20070885

Novobrantseva, T.I., A. Borodovsky, J. Wong, B. Klebanov, M. Zafari, K. Yucius, W. Querbes, P. Ge, V.M. Ruda, S. Milstein, et al. 2012. Systemic RNAi-mediated Gene Silencing in Nonhuman Primate and Rodent Myeloid Cells. *Mol Ther Nucleic Acids*. 1:e4. http://dx.doi.org/10.1038/mtna.2011.3

Panizzi, P., F.K. Swirski, J.L. Figueiredo, P. Waterman, D.E. Sosnovik, E. Aikawa, P. Libby, M. Pittet, R. Weissleder, and M. Nahrendorf. 2010. Impaired infarct healing in atherosclerotic mice with Ly-6C(hi) monocytosis. *J. Am. Coll. Cardiol.* 55:1629–1638. http://dx.doi.org/10.1016/j.jacc.2009.08.089

Qiao, J.H., J. Tripathi, N.K. Mishra, Y. Cai, S. Tripathi, X.P. Wang, S. Imes, M.C. Fishbein, S.K. Clinton, P. Libby, et al. 1997. Role of macrophage colony-stimulating factor in atherosclerosis: studies of osteopetrotic mice. *Am. J. Pathol.* 150:1687–1699.

Rajavashisth, T., J.H. Qiao, S. Tripathi, J. Tripathi, N. Mishra, M. Hua, X.P. Wang, A. Loussararian, S. Clinton, P. Libby, and A. Lusis. 1998. Heterozygous osteopetrotic (op) mutation reduces atherosclerosis in LDL receptor–deficient mice. *J. Clin. Invest.* 101:2702–2710. http://dx.doi.org/10.1172/JCI119891

Rauch, P.J., A. Chudnovskiy, C.S. Robbins, G.F. Weber, M. Etzrodt, I. Hilgendorf, E. Tiglao, J.L. Figueiredo, Y. Iwamoto, I. Theurl, et al. 2012. Innate response activator B cells protect against microbial sepsis. *Science*. 335:597–601. http://dx.doi.org/10.1126/science.1215173

Robbins, C.S., A. Chudnovskiy, P.J. Rauch, J.L. Figueiredo, Y. Iwamoto, R. Gorbatov, M. Etzrodt, G.F. Weber, T. Ueno, N. van Rooijen, et al. 2012. Extramedullary hematopoiesis generates Ly-6C(high) monocytes that infiltrate atherosclerotic lesions. *Circulation*. 125:364–374. http://dx.doi.org/10.1161/CIRCULATIONAHA.111.061986

Robbins, C.S., I. Hilgendorf, G.F. Weber, I. Theurl, Y. Iwamoto, J.L. Figueiredo, R. Gorbatov, G.K. Sukhova, L.M. Gerhardt, D. Smyth, et al. 2013. Local proliferation dominates lesional macrophage accumulation in atherosclerosis. *Nat. Med.* 19:1166–1172. http://dx.doi.org/10.1038/nm.3258

Rosas, M., L.C. Davies, P.J. Giles, C.T. Liao, B. Kharfan, T.C. Stone, V.B. O'Donnell, D.J. Fraser, S.A. Jones, and P.R. Taylor. 2014. The transcription factor Gata6 links tissue macrophage phenotype and proliferative renewal. *Science*. 344:645–648. http://dx.doi.org/10.1126/science.1251414

Salomon, R.N., R. Underwood, M.V. Doyle, A. Wang, and P. Libby. 1992. Increased apolipoprotein E and c-fms gene expression without elevated interleukin 1 or 6 mRNA levels indicates selective activation of macrophage functions in advanced human atheroma. *Proc. Natl. Acad. Sci. USA*. 89:2814–2818. http://dx.doi.org/10.1073/pnas.89.7.2814

Scott, L.M., G.V. Priestley, and T. Papayannopoulou. 2003. Deletion of alpha4 integrins from adult hematopoietic cells reveals roles in homeostasis, regeneration, and homing. *Mol. Cell. Biol.* 23:9349–9360. http://dx.doi.org/10.1128/MCB.23.24.9349-9360.2003

Shaposhnik, Z., X. Wang, and A.J. Lusis. 2010. Arterial colony stimulating factor-1 influences atherosclerotic lesions by regulating monocyte migration and apoptosis. *J. Lipid Res.* 51:1962–1970. http://dx.doi.org/10.1194/jlr.M005215

Sugiyama, T., H. Kohara, M. Noda, and T. Nagasawa. 2006. Maintenance of the hematopoietic stem cell pool by CXCL12-CXCR4 chemokine signaling in bone marrow stromal cell niches. *Immunity*. 25:977–988. http://dx.doi.org/10.1016/j.immuni.2006.10.016

Swirski, F.K., and M. Nahrendorf. 2013. Leukocyte behavior in atherosclerosis, myocardial infarction, and heart failure. *Science*. 339:161–166. http://dx.doi.org/10.1126/science.1230719

Swirski, F.K., P. Libby, E. Aikawa, P. Alcaide, F.W. Luscinskas, R. Weissleder, and M.J. Pittet. 2007. Ly-6Chi monocytes dominate hypercholesterolemia-associated monocytosis and give rise to macrophages in atheromata. *J. Clin. Invest.* 117:195–205. http://dx.doi.org/10.1172/JCI29950

Swirski, F.K., M. Nahrendorf, M. Etzrodt, M. Wildgruber, V. Cortez-Retamozo, P. Panizzi, J.L. Figueiredo, R.H. Kohler, A. Chudnovskiy, P. Waterman, et al. 2009. Identification of splenic reservoir monocytes and their deployment to inflammatory sites. *Science*. 325:612–616. http://dx.doi.org/10.1126/science.1175202

Tagliani, E., C. Shi, P. Nancy, C.S. Tay, E.G. Pamer, and A. Erlebacher. 2011. Coordinate regulation of tissue macrophage and dendritic cell population dynamics by CSF-1. *J. Exp. Med.* 208:1901–1916. http://dx.doi.org/10.1084/jem.20110866

Takahashi, K., S. Umeda, L.D. Shultz, S. Hayashi, and S. Nishikawa. 1994. Effects of macrophage colony-stimulating factor (M-CSF) on the development, differentiation, and maturation of marginal metallophilic macrophages and marginal zone macrophages in the spleen of osteopetrosis (op) mutant mice lacking functional M-CSF activity. *J. Leukoc . Biol.* 55:581–588.

Takizawa, H., R.R. Regoes, C.S. Boddupalli, S. Bonhoeffer, and M.G. Manz. 2011. Dynamic variation in cycling of hematopoietic stem cells in steady state and inflammation. *J. Exp. Med.* 208:273–284. http://dx.doi.org/10.1084/jem.20101643

Trogan, E., J.E. Feig, S. Dogan, G.H. Rothblat, V. Angeli, F. Tacke, G.J. Randolph, and E.A. Fisher. 2006. Gene expression changes in foam cells and the role of chemokine receptor CCR7 during atherosclerosis regression in ApoE-deficient mice. *Proc. Natl. Acad. Sci. USA*. 103:3781–3786. http://dx.doi.org/10.1073/pnas.0511043103

Tsujioka, H., T. Imanishi, H. Ikejima, A. Kuroi, S. Takarada, T. Tanimoto, H. Kitabata, K. Okochi, Y. Arita, K. Ishibashi, et al. 2009. Impact of heterogeneity of human peripheral blood monocyte subsets on myocardial salvage in patients with primary acute myocardial infarction. *J. Am. Coll. Cardiol.* 54:130–138. http://dx.doi.org/10.1016/j.jacc.2009.04.021

Ulyanova, T., L.M. Scott, G.V. Priestley, Y. Jiang, B. Nakamoto, P.A. Koni, and T. Papayannopoulou. 2005. VCAM-1 expression in adult hematopoietic and nonhematopoietic cells is controlled by tissue-inductive signals and reflects their developmental origin. *Blood*. 106:86–94. http://dx.doi.org/10.1182/blood-2004-09-3417

van Gils, J.M., M.C. Derby, L.R. Fernandes, B. Ramkhelawon, T.D. Ray, K.J. Rayner, S. Parathath, E. Distel, J.L. Feig, J.I. Alvarez-Leite, et al. 2012. The neuroimmune guidance cue netrin-1 promotes atherosclerosis by inhibiting the emigration of macrophages from plaques. *Nat. Immunol.* 13:136–143. http://dx.doi.org/10.1038/ni.2205

Wang, M., M. Subramanian, S. Abramowicz, A.J. Murphy, A. Gonen, J. Witztum, C. Welch, I. Tabas, M. Westerterp, and A.R. Tall. 2014. Interleukin-3/granulocyte macrophage colony-stimulating factor receptor promotes stem cell expansion, monocytosis, and atheroma macrophage burden in mice with hematopoietic ApoE deficiency. *Arterioscler. Thromb. Vasc. Biol.* 34:976–984. http://dx.doi.org/10.1161/ATVBAHA.113.303097

Williams, D.A., M. Rios, C. Stephens, and V.P. Patel. 1991. Fibronectin and VLA-4 in haematopoietic stem cell-microenvironment interactions. *Nature*. 352:438–441. http://dx.doi.org/10.1038/352438a0

Winkler, I.G., N.A. Sims, A.R. Pettit, V. Barbier, B. Nowlan, F. Helwani, I.J. Poulton, N. van Rooijen, K.A. Alexander, L.J. Raggatt, and J.P. Lévesque. 2010. Bone marrow macrophages maintain hematopoietic stem cell (HSC) niches and their depletion mobilizes HSCs. *Blood*. 116:4815–4828. http://dx.doi.org/10.1182/blood-2009-11-253534

Yona, S., K.W. Kim, Y. Wolf, A. Mildner, D. Varol, M. Breker, D. Strauss-Ayali, S. Viukov, M. Guilliams, A. Misharin, et al. 2013. Fate mapping reveals origins and dynamics of monocytes and tissue macrophages under homeostasis. *Immunity*. 38:79–91. http://dx.doi.org/10.1016/j.immuni.2012.12.001